

# Low-Complexity Signal Detection for Large-Scale MIMO in Optical Wireless Communications

Xinyu Gao, *Student Member, IEEE*, Linglong Dai, *Senior Member, IEEE*, Yuting Hu, *Student Member, IEEE*, Yu Zhang, *Senior Member, IEEE*, and Zhaocheng Wang, *Senior Member, IEEE*

**Abstract**—Optical wireless communication (OWC) has been a rapidly growing research area in recent years. Applying multiple-input multiple-output (MIMO), particularly large-scale MIMO, into OWC is very promising to substantially increase spectrum efficiency. However, one challenging problem to realize such an attractive goal is the practical signal detection algorithm for optical MIMO systems, whereby the linear signal detection algorithm like minimum mean square error (MMSE) can achieve satisfying performance but involves complicated matrix inversion of large size. In this paper, we first prove a special property that the filtering matrix of the linear MMSE algorithm is symmetric positive definite for indoor optical MIMO systems. Based on this property, a low-complexity signal detection algorithm based on the successive overrelaxation (SOR) method is proposed to reduce the overall complexity by one order of magnitude with a negligible performance loss. The performance guarantee of the proposed SOR-based algorithm is analyzed from the following three aspects. First, we prove that the SOR-based algorithm is convergent for indoor large-scale optical MIMO systems. Second, we prove that the SOR-based algorithm with the optimal relaxation parameter can achieve a faster convergence rate than the recently proposed Neumann-based algorithm. Finally, a simple quantified relaxation parameter, which is independent of the receiver location and signal-to-noise ratio, is proposed to guarantee the performance of the SOR-based algorithm in practice. Simulation results verify that the proposed SOR-based algorithm can achieve the exact performance of the classical MMSE algorithm with a small number of iterations.

**Index Terms**—Optical wireless communications, large-scale MIMO, signal detection, minimum mean square error (MMSE), low complexity.

## I. INTRODUCTION

OPTICAL wireless communication (OWC) like visible light communication with huge spectrum has recently drawn increasing attention, since it can significantly relieve the crowded radio frequency (RF) spectrum [1], [2] and enable attractively high speed data transmission, especially for indoor scenarios [3]. As the wavelength of visible light is very small

(about 400 nm ~ 700 nm), and the indoor applications can provide high signal-to-noise ratio (SNR) [4], it is very promising to apply the well-established multiple-input multiple-output (MIMO) technique in RF systems [5], or even the recently proposed large-scale MIMO using tens or hundreds of antennas [6], into indoor OWC to simultaneously increase the spectrum efficiency and energy efficiency by orders of magnitude [7].

Unlike traditional RF MIMO systems, indoor optical MIMO systems employ multiple arrays of energy-efficient illumination devices (e.g., light emitting diodes (LEDs)) in the ceiling as the transmit antennas, and the receiver with multiple photodetectors serving as the receive antennas. Although correlation exists among the indoor optical MIMO channels due to the fact that indoor propagation environments usually do not have obvious fading effects caused by turbulence [5], [8], some feasible optical MIMO system realizations have already been proposed to overcome this problem so that the expected gain by employing MIMO can be achieved, e.g., [4] and [5] respectively propose to use an imaging receiver and a link blockage to reduce the MIMO channel correlation and hence a full-rank channel matrix can be guaranteed.

One of the remaining challenging problems to realize the attractive spectrum efficiency of optical MIMO systems is the practical signal detection algorithm [9]. Similar to RF MIMO systems, the optimal signal detector for optical MIMO systems using intensity modulation and direct detection (IM/DD) is the maximum likelihood (ML) detector [10], but its complexity increases exponentially with the number of LED arrays, which makes it impractical for large-scale optical MIMO systems. To achieve the (close) optimal ML detection performance with reduced complexity, some non-linear signal detection algorithms have been proposed. One typical category is based on the sphere decoding (SD) algorithm [11], such as the fixed-complexity sphere decoding (FSD) [12]. This kind of algorithm uses the underlying lattice structure of the received signal and considers the most promising approach to achieve the ML detection performance with reduced complexity. It performs well for conventional small-scale MIMO systems, but when the dimension of the MIMO systems becomes large (e.g., 36 LED arrays [4]), the complexity is still unaffordable. Another typical category is based on the tabu search (TS) algorithm derived from artificial intelligence, such as the layered tabu search (LTS) algorithm [13] and the random-restart reactive tabu search (3RTS) algorithm [14]. This kind of algorithm utilizes the idea of local neighborhood search to estimate the transmitted signal, and limits the selection of neighborhood by a tabu list. When the range of neighborhood is appropriately

Manuscript received May 28, 2014; revised April 25, 2015; accepted July 11, 2015. Date of publication July 15, 2015; date of current version August 17, 2015. This work was supported in part by the International Science & Technology Cooperation Program of China (Grant No. 2015DFG12760), the National Natural Science Foundation of China (Grant No. 61201185 and 61271266), the Beijing Natural Science Foundation (Grant No. 4142027), and the Foundation of Shenzhen government. (*Corresponding author: Linglong Dai.*)

The authors are with Tsinghua National Laboratory for Information Science and Technology (TNList), Department of Electronic Engineering, Tsinghua University, Beijing 100084, China (e-mail: gxy1231992@sina.com; dai11@tsinghua.edu.cn; 740733663@qq.com; zhang-yu@tsinghua.edu.cn; zcwang@tsinghua.edu.cn).

Color versions of one or more of the figures in this paper are available online at <http://ieeexplore.ieee.org>.

Digital Object Identifier 10.1109/JSAC.2015.2457211

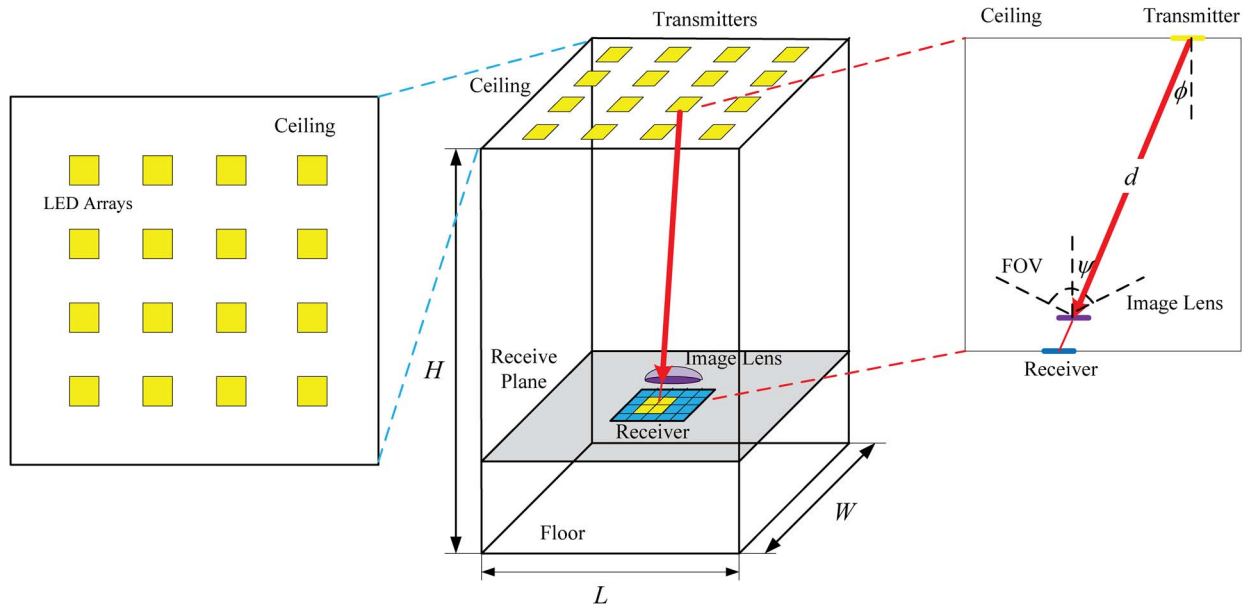


Fig. 1. Indoor optical MIMO system model with an imaging receiver.

small and the tabu list is carefully designed, the complexity is acceptable for large-scale MIMO systems, but it suffers from a non-negligible performance loss compared to the optimal ML detector.

To make a trade-off between the performance and complexity, one can resort to linear signal detection algorithms such as zero-forcing (ZF) and minimum mean square error (MMSE), which have already been used for indoor IM/DD optical MIMO systems [3]–[5], [8]. However, these linear algorithms involve unfavorable matrix inversion of a large size. Very recently, the Neumann series approximation algorithm [15] (which is called as Neumann-based algorithm in this paper) has been proposed to convert the matrix inversion into a series of matrix-vector multiplications, so the complexity for signal detection can be reduced, but only a marginal reduction in complexity can be achieved.

In this paper, we propose a signal detection algorithm based on the successive overrelaxation (SOR) method [16] to reduce the computational complexity without performance loss. Specifically, the contributions of this paper can be summarized as follows:

- (1) We prove a special property that the MMSE filtering matrix to be inverted is symmetric positive definite for indoor large-scale optical MIMO systems, which is the premise to employ the SOR method.
- (2) We propose SOR-based algorithm to detect the transmitted signal in an iterative way without the complicated matrix inversion, and the complexity analysis shows that the overall complexity for signal detection can be reduced by one order of magnitude.
- (3) We prove the convergence of SOR-based algorithm to guarantee its feasibility by exploiting the definition of eigenvalue. The convergence rate analysis is provided to show that SOR-based algorithm with the optimal relaxation parameter can converge faster than the recently proposed Neumann-based algorithm [15]. We also pro-

pose a simple quantified relaxation parameter, which is independent of the receiver location and signal-to-noise ratio (SNR), to guarantee the performance of SOR-based algorithm in practice.

- (4) We conduct extensive simulations to demonstrate that SOR-based algorithm without the complicated matrix inversion can achieve the exact performance of the classical MMSE algorithm for indoor large-scale optical MIMO systems with a small number of iterations, even when the receiver is located near the room edges.

The rest of the paper is organized as follows: Section II briefly describes the system model of indoor large-scale optical MIMO. Section III specifies the proposed low-complexity signal detection algorithm, together with the performance analysis. The simulation results of the bit error rate (BER) performance are provided in Section IV. Finally, conclusions are drawn in Section V.

*Notation:* We use lower-case and upper-case boldface letters to denote vectors and matrices, respectively;  $(\cdot)^T$ ,  $(\cdot)^H$ ,  $(\cdot)^{-1}$ , and  $|\cdot|$  denote the transpose, conjugate transpose, matrix inversion, and absolute operators, respectively;  $\|\cdot\|_F$  and  $\|\cdot\|_2$  denote the Frobenius norm of a matrix and the 2-norm of a vector, respectively; Finally,  $\mathbf{I}_N$  represents the  $N \times N$  identity matrix.

## II. SYSTEM MODEL

As illustrated in Fig. 1, we consider a typical IM/DD indoor optical MIMO system in a room with the dimension  $L \times W \times H$  [4], where  $N_t$  LED arrays are installed in the ceiling as the transmit antennas, and  $N_r$  photodetectors are employed as the receive antennas. To ensure the channel spatial diversity, an imaging receiver, which can project an image of each LED array on a larger number of photodetectors (i.e.,  $N_r$  is usually larger than  $N_t$ ), is used [17]. It is worth noting that the

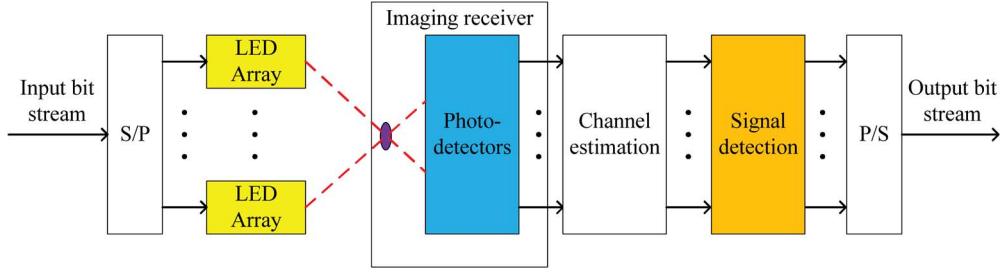


Fig. 2. The overall diagram of the optical MIMO system.

dimension of indoor optical MIMO is usually large to achieve a satisfied data rate [4].

Fig. 2 shows the overall diagram of the optical MIMO system. The serial transmitted bits are first parallelized into  $N_t$  streams by a serial-to-parallel converter (S/P), and then transmitted by the LED arrays. Let  $\mathbf{s} = [s_1, \dots, s_{N_t}]^T$  denote the transmitted signal vector which contains the transmitted bits from all  $N_t$  LED arrays, and  $\mathbf{H}$  denote the  $N_r \times N_t$  optical MIMO channel matrix, then the received signal vector  $\mathbf{y} = [y_1, \dots, y_{N_r}]^T$  at the receiver can be represented as

$$\mathbf{y} = \mathbf{H}\mathbf{s} + \mathbf{n}, \quad (1)$$

where  $\mathbf{n} = [n_1, \dots, n_{N_r}]^T$  is the noise vector whose major component is the thermal noise compared to the ambient shot light noise [18], whose elements are independent and identically distributed (i.i.d.) following the distribution  $\mathcal{N}(0, \sigma^2)$  [4].

For indoor visible light communications, it has been widely reported that the power of the diffusing component caused by the reflection from the surfaces of the room is much lower than that of the line-of-sight (LOS) component, even when the receiver is located near the room edges [5], [19]. Thus, usually the LOS component is considered in the literature [4], [5], [19], and we also consider the LOS component in this paper, where the element  $h_{ij}$  of the channel matrix  $\mathbf{H}$  at the  $i$ th row and  $j$ th column can be presented as [4], [18]

$$h_{ij} = a_{ij}h_i, \quad (2)$$

where  $h_i$  presents the normalized power in the image projected from the  $i$ th LED array to the aperture of image lens when the imaging receiver is located at a particular position, and it can be expressed as

$$h_i = \begin{cases} \sum_{k=1}^{K_i} \frac{(m+1)A_R}{2\pi d_{ik}^2} \cos^m(\phi_{ik}) \cos(\psi_{ik}) T_s(\psi_{ik}) G(\psi_{ik}), & \text{if } |\psi_{ik}| < \psi_c, \\ 0, & \text{if } |\psi_{ik}| > \psi_c, \end{cases} \quad (3)$$

where  $K_i$  denotes the number of LEDs in the  $i$ th array;  $m = \frac{-\ln 2}{\ln(\cos(\phi_{1/2}))}$  presents the order of Lambertian emission, where  $\phi_{1/2}$  is the emission semi-angle of an LED;  $A_R$  presents the physical area of the imaging receiver;  $d_{ik}$  is the distance between the  $k$ th LED in the  $i$ th array and the center of the image lens;  $\phi_{ik}$  and  $\psi_{ik}$  denote the angle of emission and incidence, respectively;  $\psi_c$  presents the width of the field of vision (FOV)

at the imaging receiver;  $T_s(\psi_{ik})$  is the optical filter gain which is set as one without loss of generality [18]. Finally,  $G(\psi_{ik})$  denotes the gain of the optical concentrator, which can be presented as

$$G(\psi_{ik}) = \begin{cases} \frac{n^2}{\sin^2(\phi_{1/2})}, & |\psi_{ik}| < \phi_{1/2}, \\ 0, & |\psi_{ik}| > \phi_{1/2}, \end{cases} \quad (4)$$

where  $n$  is the refractive index of the optical concentrator material.

The other component  $a_{ij}$  of  $h_{ij}$  in (2) presents the proportion of received power of the imaging receiver falling on the  $j$ th photodetector, which can be presented as

$$a_{ij} = \frac{A_{ij}}{\sum_{l=1}^{N_r} A_{il}}, \quad (5)$$

where  $A_{ij}$  denotes the area of image of the  $i$ th array on the  $j$ th photodetector. Note that a specific method to determine the position size of the images can be found in [4].

At the receiver, after the channel matrix  $\mathbf{H}$  has been obtained through time-domain and/or frequency-domain training pilots [20], [21], the task of signal detection is to recover the transmitted signal vector  $\mathbf{s}$  from the received signal vector  $\mathbf{y}$ . To make a trade-off between the performance and the complexity, the classical MMSE linear signal detection algorithm has been widely used for indoor optical MIMO systems [3]–[5], and the estimate of the transmitted signal vector  $\hat{\mathbf{s}}$  can be obtained by

$$\hat{\mathbf{s}} = (\mathbf{H}^H \mathbf{H} + \sigma^2 \mathbf{I}_{N_t})^{-1} \mathbf{H}^H \mathbf{y} = \mathbf{W}^{-1} \hat{\mathbf{y}}, \quad (6)$$

where  $\hat{\mathbf{y}} = \mathbf{H}^H \mathbf{y}$  can be interpreted as the matched-filter output of the received signal  $\mathbf{y}$ , and the MMSE filtering matrix  $\mathbf{W}$  is denoted as

$$\mathbf{W} = \mathbf{G} + \sigma^2 \mathbf{I}_{N_t}, \quad (7)$$

where  $\mathbf{G} = \mathbf{H}^H \mathbf{H}$  is the Gram matrix. The computational complexity of the exact matrix inversion  $\mathbf{W}^{-1}$  is  $\mathcal{O}(N_t^3)$ , which is high for indoor large-scale optical MIMO systems in practice [4].

After signal detection, the transmitted bits are recovered [22] and then converted into a serial stream by a parallel-to-serial converter (P/S).

### III. LOW-COMPLEXITY SIGNAL DETECTION FOR INDOOR LARGE-SCALE OPTICAL MIMO SYSTEMS

In this section, we first prove a special property of indoor optical MIMO systems that the MMSE filtering matrix is symmetric positive definite. Based on this property, we propose a low-complexity SOR-based signal detection algorithm to iteratively achieve the performance of MMSE algorithm without matrix inversion. The convergence proof of the proposed algorithm is then derived. We also prove that SOR-based algorithm with the optimal relaxation parameter can converge faster than the recently proposed Neumann-based algorithm. After that, a simple quantified relaxation parameter is proposed to guarantee the performance of SOR-based algorithm in practice. Finally, the complexity analysis of SOR-based algorithm is provided to show its advantages over conventional schemes.

#### A. Signal Detection Algorithm Based on SOR Method

Recently, Neumann-based algorithm [15] is proposed as an efficient signal detection algorithm in large-scale MIMO systems, as it can convert the complicated matrix inversion into a series of matrix-vector multiplications together with a very small number of divisions to reduce the complexity. Neumann-based algorithm detects the transmitted signal vector  $\mathbf{s}$  as

$$\hat{\mathbf{s}}_N^{(i+1)} = \sum_{k=0}^i \left( -\mathbf{D}^{-1}(\mathbf{L} + \mathbf{L}^T) \right)^k \mathbf{D}^{-1}, \quad (8)$$

where the superscript  $i = 0, 1, 2, \dots$  denotes the number of iterations,  $\mathbf{D}$ ,  $\mathbf{L}$ , and  $\mathbf{L}^T$  are the diagonal component, the strictly lower triangular component, and the strictly upper triangular component of  $\mathbf{W}$ , respectively, which satisfy

$$\mathbf{W} = \mathbf{D} + \mathbf{L} + \mathbf{L}^T, \quad (9)$$

where

$$\mathbf{D} = \begin{bmatrix} w_{1,1} & 0 & \cdots & 0 \\ 0 & w_{2,2} & \cdots & 0 \\ \vdots & \vdots & \ddots & \vdots \\ 0 & 0 & \cdots & w_{N_r, N_r} \end{bmatrix}, \quad (10)$$

$$\mathbf{L} = \begin{bmatrix} 0 & 0 & \cdots & 0 \\ w_{2,1} & 0 & \cdots & 0 \\ \vdots & \vdots & \ddots & \vdots \\ w_{N_r, 1} & w_{N_r, 2} & \cdots & 0 \end{bmatrix}, \quad (11)$$

where  $w_{i,j}$  denotes the element of  $\mathbf{W}$  in the  $i$ th row and  $j$ th column. The iteration matrix  $\mathbf{B}_N$  of Neumann-based algorithm can be presented as  $\mathbf{B}_N = \mathbf{D}^{-1}(\mathbf{L} + \mathbf{L}^T) = \mathbf{D}^{-1}\mathbf{W} - \mathbf{I}_{N_r}$ . It has been proved that Neumann-based algorithm can converge when  $N_r$  is much larger than  $N_t$  (e.g.,  $N_r/N_t = 32$  [15]). However, for a more realistic system, it cannot converge fast and only a marginal reduction in complexity can be achieved.

To solve this problem, in this paper, we propose a low-complexity SOR-based algorithm by utilizing the special property that the MMSE filtering matrix is symmetric positive definite for indoor optical MIMO systems, as proved by the following **Lemma 1**.

*Lemma 1:* For indoor optical MIMO systems using imaging receiver, the MMSE filtering matrix  $\mathbf{W}$  is symmetric positive definite.

*Proof:* As all the elements of the channel matrix  $\mathbf{H}$  are real for the IM/DD optical MIMO systems, the transpose of matrix and the conjugate transpose of matrix will be the same, e.g.,  $\mathbf{G} = \mathbf{H}^H \mathbf{H} = \mathbf{H}^T \mathbf{H}$ . Then, we have

$$\mathbf{W}^T = (\mathbf{G} + \sigma^2 \mathbf{I}_{N_t})^T = \mathbf{W}, \quad (12)$$

which indicates that the MMSE filtering matrix  $\mathbf{W}$  is symmetric. Meanwhile, for indoor optical MIMO systems with imaging receiver, the channel matrix  $\mathbf{H}$  has full column rank [4], i.e., the equation  $\mathbf{H}\mathbf{q} = \mathbf{0}$  has a unique solution, which is the  $N_t \times 1$  zero vector. Thus, for any  $N_t \times 1$  non-zero real-valued vector  $\mathbf{r}$ , we have

$$\mathbf{r}^T \mathbf{W} \mathbf{r} = \mathbf{r}^T (\mathbf{G} + \sigma^2 \mathbf{I}_{N_t}) \mathbf{r} > 0, \quad (13)$$

which implies that  $\mathbf{W}$  is positive definite. Considering (12) and (13), we can conclude that the MMSE filtering matrix  $\mathbf{W} = \mathbf{G} + \sigma^2 \mathbf{I}_{N_t}$  (7) is symmetric positive definite.  $\square$

The special property that the MMSE filtering matrix  $\mathbf{W}$  for indoor optical MIMO systems is symmetric positive definite inspires us to exploit the SOR method to efficiently solve (6) with low complexity. The SOR method is used to solve the  $N$ -dimension linear equation  $\mathbf{A}\mathbf{x} = \mathbf{b}$ , where  $\mathbf{A}$  is the  $N \times N$  symmetric positive definite matrix,  $\mathbf{x}$  is the  $N \times 1$  solution vector, and  $\mathbf{b}$  is the  $N \times 1$  measurement vector. Unlike the traditional method that directly computes  $\mathbf{A}^{-1}\mathbf{b}$  to obtain  $\mathbf{x}$ , the SOR method can efficiently solve the linear equation  $\mathbf{A}\mathbf{x} = \mathbf{b}$  in an iterative manner without the complicated matrix inversion [16]. Since the MMSE filtering matrix  $\mathbf{W}$  is also symmetric positive definite for indoor optical MIMO systems as proved in **Lemma 1**, we can utilize the SOR method to estimate the transmitted signal vector  $\mathbf{s}$  as below

$$\left( \mathbf{L} + \frac{1}{\gamma} \mathbf{D} \right) \hat{\mathbf{s}}^{(i+1)} = \hat{\mathbf{y}} + \left( \left( \frac{1}{\gamma} - 1 \right) \mathbf{D} - \mathbf{L}^T \right) \hat{\mathbf{s}}^{(i)}, \quad (14)$$

where the definitions of  $\mathbf{D}$ ,  $\mathbf{L}$ , and  $\mathbf{L}^T$  are the same as that in (9),  $\gamma$  represents the relaxation parameter, which plays an important role in the convergence and the convergence rate as will be discussed in the following Section III-B and Section III-C, respectively,  $\hat{\mathbf{s}}^{(0)}$  denotes the initial solution, which is usually set as an  $N_t \times 1$  zero vector without loss of generality due to no priori information of the final solution is available [16]. Such initial solution will not affect the convergence of the proposed SOR-based algorithm as we will prove in the following **Lemma 2**. Consequently, the final accuracy will also not be affected by the initial solution if the number of iterations  $i$  is relatively large (e.g.,  $i = 4$  as will be verified later by simulation results in Section IV).

#### B. Convergence Proof

*Lemma 2:* For indoor optical MIMO systems, SOR-based algorithm is convergent, when the relaxation parameter  $\gamma$  satisfies  $0 < \gamma < 2$  for any initial solution.

*Proof:* We define  $\mathbf{B}_S = \left(\mathbf{L} + \frac{1}{\gamma}\mathbf{D}\right)^{-1} \left(\frac{1}{\gamma}\mathbf{D} - \mathbf{D} - \mathbf{L}^T\right)$  as the iteration matrix of SOR-based algorithm, and  $\mathbf{d} = \left(\mathbf{L} + \frac{1}{\gamma}\mathbf{D}\right)^{-1} \hat{\mathbf{y}}$ . Then SOR-based algorithm (14) can be rewritten as

$$\hat{\mathbf{s}}^{(i+1)} = \mathbf{B}_S \hat{\mathbf{s}}^{(i)} + \mathbf{d}. \quad (15)$$

We call the iteration procedure is convergent if the generated sequences  $\{\hat{\mathbf{s}}^{(i)}\}$  (for  $i = 0, 1, 2, \dots$ ) converge for any initial vector  $\hat{\mathbf{s}}^{(0)}$ . It follows that if (15) converges, we have  $\lim_{i \rightarrow \infty} \hat{\mathbf{s}}^{(i)} = \hat{\mathbf{s}}$ , then  $\hat{\mathbf{s}}$  satisfies  $\hat{\mathbf{s}} = \mathbf{B}_S \hat{\mathbf{s}} + \mathbf{d}$ , and hence  $\hat{\mathbf{s}}$  is the final solution, i.e., the detection result of MMSE algorithm (6).

The spectral radius of the iteration matrix  $\mathbf{B}_S \in \mathbb{R}^{N_t \times N_t}$  is defined as the non-negative number  $\rho(\mathbf{B}_S) = \max_{1 \leq n \leq N_t} |\lambda_n|$ , where  $\lambda_n$  denotes the  $n$ th eigenvalue of  $\mathbf{B}_S$ . The necessary and sufficient conditions for the convergence of (15) is that the spectral radius  $\rho(\mathbf{B}_S)$  should satisfy [16, Theorem 7.2.2]

$$\rho(\mathbf{B}_S) = \max_{1 \leq n \leq N_t} |\lambda_n| < 1. \quad (16)$$

According to the definition of eigenvalue, we have

$$\mathbf{B}_S \mathbf{r} = \left(\mathbf{L} + \frac{1}{\gamma}\mathbf{D}\right)^{-1} \left(\frac{1}{\gamma}\mathbf{D} - \mathbf{D} - \mathbf{L}^T\right) \mathbf{r} = \lambda_n \mathbf{r}, \quad (17)$$

where  $\mathbf{r}$  is the  $N_t \times 1$  corresponding eigenvector. Note that (17) can be also presented as

$$\left(\frac{1}{\gamma}\mathbf{D} - \mathbf{D} - \mathbf{L}^T\right) \mathbf{r} = \left(\mathbf{L} + \frac{1}{\gamma}\mathbf{D}\right) \lambda_n \mathbf{r}. \quad (18)$$

Multiply both sides of (18) by  $\mathbf{r}^T$  will yield

$$\mathbf{r}^T \left(\frac{1}{\gamma}\mathbf{D} - \mathbf{D} - \mathbf{L}^T\right) \mathbf{r} = \lambda_n \mathbf{r}^T \left(\mathbf{L} + \frac{1}{\gamma}\mathbf{D}\right) \mathbf{r}. \quad (19)$$

Then we take transpose on both sides of (19), and another equation can be obtained as

$$\mathbf{r}^T \left(\frac{1}{\gamma}\mathbf{D} - \mathbf{D} - \mathbf{L}\right) \mathbf{r} = \lambda_n \mathbf{r}^T \left(\mathbf{L}^T + \frac{1}{\gamma}\mathbf{D}\right) \mathbf{r}. \quad (20)$$

Note that  $\mathbf{D} = \mathbf{D}^T$  as  $\mathbf{D}$  is a diagonal matrix. Add (19) and (20) will lead to

$$\mathbf{r}^T \left( \left(\frac{2}{\gamma} - 2\right) \mathbf{D} - \mathbf{L} - \mathbf{L}^T \right) \mathbf{r} = \lambda_n \mathbf{r}^T \left( \mathbf{L}^T + \mathbf{L} + \frac{2}{\gamma} \mathbf{D} \right) \mathbf{r}. \quad (21)$$

Substituting (9) into (21), we have

$$(1 - \lambda_n) \left(\frac{2}{\gamma} - 1\right) \mathbf{r}^T \mathbf{D} \mathbf{r} = (1 + \lambda_n) \mathbf{r}^T \mathbf{W} \mathbf{r}. \quad (22)$$

Since the MMSE filtering matrix  $\mathbf{W}$  is positive definite as proved in **Lemma 1**, the diagonal matrix  $\mathbf{D}$  is positive definite, too. Then we have  $\mathbf{r}^T \mathbf{D} \mathbf{r} > 0$  and  $\mathbf{r}^T \mathbf{W} \mathbf{r} > 0$ . Besides, we also have  $\left(\frac{2}{\gamma} - 1\right) > 0$  if  $0 < \gamma < 2$ . Thus, we can conclude that  $(1 - \lambda_n)(1 + \lambda_n) > 0$ , which means

$$|\lambda_n| < 1. \quad (23)$$

Substituting (23) into (16), we can assert that  $\rho(\mathbf{B}_S) < 1$ , so SOR-based algorithm (14) is convergent.  $\square$

It is worth pointing out that another different proof of **Lemma 2** can be found in [23, Theorem 11.2.3], which utilizes the orthogonal transformation with high complexity to obtain the convergence proof, while our method directly exploits the definition of eigenvalue, which is simpler than the existing method [23].

### C. Convergence Rate Analysis

In this part, we first prove that SOR-based algorithm with the optimal relaxation parameter can achieve a faster convergence rate than Neumann-based algorithm [15]. After that, we propose a simple quantified relaxation parameter independent of the receiver location and SNR, which can still guarantee the performance of SOR-based algorithm.

From (14), we can observe that the approximation error induced by SOR-based algorithm can be presented as

$$\hat{\mathbf{s}}^{(i+1)} - \hat{\mathbf{s}} = \mathbf{B}_S \left(\hat{\mathbf{s}}^{(i)} - \hat{\mathbf{s}}\right) = \dots = \mathbf{B}_S^{(i+1)} \left(\hat{\mathbf{s}}^{(0)} - \hat{\mathbf{s}}\right), \quad (24)$$

where  $\mathbf{B}_S = \left(\mathbf{L} + \frac{1}{\gamma}\mathbf{D}\right)^{-1} \left(\frac{1}{\gamma}\mathbf{D} - \mathbf{D} - \mathbf{L}^T\right)$  is the iteration matrix of SOR-based algorithm. Without loss of generality, we can utilize the 2-norm to evaluate the approximation error as [16]

$$\left\| \hat{\mathbf{s}}^{(i+1)} - \hat{\mathbf{s}} \right\|_2 = \left\| \mathbf{B}_S^{(i+1)} \right\|_F \left\| \hat{\mathbf{s}}^{(0)} - \hat{\mathbf{s}} \right\|_2. \quad (25)$$

Since  $\left\| \hat{\mathbf{s}}^{(0)} - \hat{\mathbf{s}} \right\|_2$  is a constant parameter independent of the number of iterations  $i$  after the initial solution  $\hat{\mathbf{s}}^{(0)}$  has been selected as a zero-vector, we can observe from (25) that the convergence rate achieved by SOR-based algorithm is mainly affected by  $\left\| \mathbf{B}_S^{(i+1)} \right\|_F$ .

According to the definition of  $\mathbf{B}_S$ ,  $\left\| \mathbf{B}_S^{(i+1)} \right\|_F$  is heavily related to the relaxation parameter  $\gamma$ , so there exists an optimal  $\gamma_{\text{opt}}$  to minimize  $\left\| \mathbf{B}_S^{(i+1)} \right\|_F$ , or equivalently maximize the convergence rate as shown in (25). However, it is not easy to derive a close-form relationship between  $\left\| \mathbf{B}_S^{(i+1)} \right\|_F$  and  $\gamma$ . To solve this problem, we convert this difficult optimization problem into an equivalent one that is easier to be handled by exploiting the fact that  $\left\| \mathbf{B}_S^{(i+1)} \right\|_F \approx \rho^{(i+1)}(\mathbf{B}_S)$ , where  $i$  is relatively large and  $\rho(\mathbf{B}_S) = \max_{1 \leq n \leq N_t} |\lambda_n|$  is the spectral radius of the iteration matrix  $\mathbf{B}_S$  [16]. Then, to achieve the fastest convergence rate will be equivalent to achieve the smallest  $\rho(\mathbf{B}_S)$  by selecting the optimal relaxation parameter  $\gamma_{\text{opt}}$  as

$$\gamma_{\text{opt}} = \arg \min_{0 < \gamma < 2} \rho(\mathbf{B}_S),$$

$$\text{s.t. } \mathbf{B}_S = \left(\mathbf{L} + \frac{1}{\gamma}\mathbf{D}\right)^{-1} \left(\frac{1}{\gamma}\mathbf{D} - \mathbf{D} - \mathbf{L}^T\right). \quad (26)$$

Here, we first derive the solution to (26) by assuming the channel is a Rayleigh fading channel. Then, we provide the analysis to show that similar results still hold for indoor

large-scale optical MIMO systems. After that, a simple yet efficient selection of the relaxation parameter  $\gamma$  is proposed.

For large-scale MIMO systems in Rayleigh fading channels, we usually have  $N_r \gg N_t$  (e.g.,  $N_r/N_t = 16$  [24]), so the column vectors of the channel matrix  $\mathbf{H}$  are asymptotically orthogonal according to the random matrix theory [25], leading to the MMSE filtering matrix  $\mathbf{W} = \mathbf{G} + \sigma^2 \mathbf{I}_{N_r}$  (7) to be a diagonal dominant matrix. For such systems, it has been proved in [26] that the spectral radius  $\rho(\mathbf{B}_S)$  of the iteration matrix  $\mathbf{B}_S$  satisfies

$$(\rho(\mathbf{B}_S) + \gamma - 1)^2 = \gamma^2 \rho^2(\mathbf{B}_N) \rho(\mathbf{B}_S), \quad (27)$$

where  $\rho(\mathbf{B}_N)$  is the spectral radius of the iteration matrix  $\mathbf{B}_N$  of Neumann-based algorithm (8). Note that for large-scale MIMO systems in Rayleigh fading channels, we have  $\rho(\mathbf{B}_N) < 1$  [15]. Then, by combining (26) and (27), we can obtain the optimal relaxation parameter  $\gamma_{\text{opt}}$  as

$$\gamma_{\text{opt}} = \frac{2}{\sqrt{1 - \rho^2(\mathbf{B}_N)} + 1}. \quad (28)$$

Substituting (28) into (27), we can attain the optimal spectral radius  $\rho(\mathbf{B}_S)$  as  $\rho(\mathbf{B}_S) = \gamma_{\text{opt}} - 1$ . Based on (28), we can also conclude that SOR-based algorithm with the optimal relaxation parameter  $\gamma_{\text{opt}}$  enjoys a faster convergence rate than Neumann-based algorithm as will be proved by the following **Lemma 3**.

**Lemma 3:** For large-scale MIMO systems in Rayleigh fading channels, SOR-based algorithm with the optimal relaxation parameter  $\gamma_{\text{opt}}$  enjoys a faster convergence rate than Neumann-based algorithm, i.e.,  $\rho(\mathbf{B}_S) < \rho(\mathbf{B}_N)$ .

*Proof:* Based on the analysis above, when  $\gamma = \gamma_{\text{opt}}$  is selected, we have

$$\rho(\mathbf{B}_S) = \frac{2}{\sqrt{1 - \rho^2(\mathbf{B}_N)} + 1} - 1, \quad (29)$$

where  $0 < \rho(\mathbf{B}_N) < 1$ . To prove  $\rho(\mathbf{B}_S) < \rho(\mathbf{B}_N)$ , we can first consider two functions of  $\rho(\mathbf{B}_N)$ . The first one is  $f_1 = \sqrt{1 - \rho^2(\mathbf{B}_N)}$ , which can be regarded as the point on the unit circle in the Cartesian coordinate system. The second one is  $f_2 = \frac{2}{1 + \rho(\mathbf{B}_N)} - 1$ , which can be interpreted as the point on a hyperbolic curve. Since  $0 < \rho(\mathbf{B}_N) < 1$ , we can assert that  $f_2 < f_1$ , then the following inequality can be drawn

$$\rho(\mathbf{B}_S) = \frac{2}{\sqrt{1 - \rho^2(\mathbf{B}_N)} + 1} - 1 < \rho(\mathbf{B}_N). \quad (30)$$

□

Next, we try to quantify the optimal relaxation parameter  $\gamma_{\text{opt}}$ . Note that for large-scale MIMO systems in Rayleigh fading channels, the diagonal matrix  $\mathbf{D}$  can be well approximated by  $(N_r + \sigma^2) \mathbf{I}_{N_r}$ , and the largest eigenvalue of the MMSE filtering matrix can be estimated as  $N_r (1 + \sqrt{N_t/N_r})^2 + \sigma^2$  with a small error [25]. Then, we can conclude that

$$\begin{aligned} \rho(\mathbf{B}_N) &\approx \frac{N_r (1 + \sqrt{N_t/N_r})^2 + \sigma^2}{N_r + \sigma^2} - 1 \\ &\approx (1 + \sqrt{N_t/N_r})^2 - 1, \end{aligned} \quad (31)$$

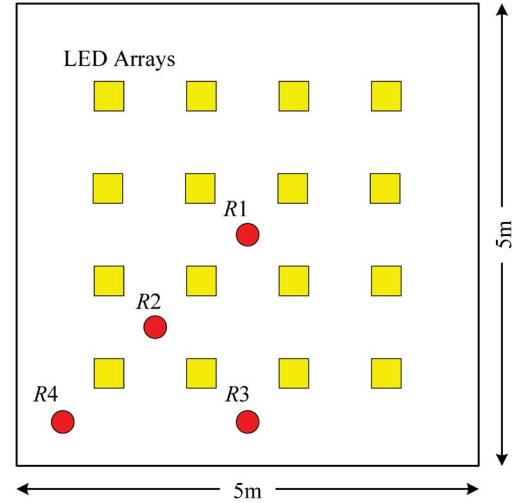


Fig. 3. The receiver is located at different places  $R1$ ,  $R2$ ,  $R3$ , and  $R4$  within the room.

where the second approximation is valid due to the fact that  $N_r$  is usually much larger than the noise power  $\sigma^2$ . Then, substituting (31) into (28), we have

$$\bar{\gamma}_{\text{opt}} = \frac{2}{\sqrt{1 - a^2} + 1}, \quad (32)$$

where  $a = (1 + \sqrt{N_t/N_r})^2 - 1$ , and  $\bar{\gamma}_{\text{opt}}$  is the quantified value of the optimal relaxation parameter  $\gamma_{\text{opt}}$  with a negligible error.

Next, we consider indoor large-scale optical MIMO systems with imaging receivers. For such systems as described in Section II, it can still be guaranteed that the column vectors of the channel matrix  $\mathbf{H}$  are asymptotically orthogonal by carefully designing the image lens of the receiver [19], [27], even for the system where  $N_r/N_t$  is not very large and the position of the receiver is near the room edges. Therefore, the conclusions including (28) and **Lemma 3** still hold for indoor large-scale optical MIMO systems. Moreover, for the same dimension of MIMO system where  $N_r/N_t$  is not very large, the indoor large-scale optical MIMO channel with imaging receivers can be designed to be more close to the preferred column orthogonality. Then, the elements of the diagonal matrix  $\mathbf{D}$  will be larger, while the elements of the strictly lower triangular matrix  $\mathbf{L}$  will be smaller. Therefore, we can conclude that  $\rho(\mathbf{B}_N)$  can be upper bounded by the deterministic parameter  $a$  in (32) as  $\rho(\mathbf{B}_N) < a$ . As a result, based on (28), the optimal relaxation parameter  $\gamma_{\text{opt}}$  for the indoor large-scale optical MIMO systems is limited to the range  $1 < \gamma_{\text{opt}} < \frac{2}{\sqrt{1 - a^2} + 1}$ . Since  $N_r$  is usually larger than  $N_t$ , e.g.,  $N_t \times N_r = 16 \times 144$  [4], the upper bound  $\frac{2}{\sqrt{1 - a^2} + 1}$  of  $\gamma_{\text{opt}}$  is close to 1. Then, an appropriate  $\gamma$  can be simply chosen as

$$\gamma = \frac{1}{2} \left( 1 + \frac{2}{\sqrt{1 - a^2} + 1} \right). \quad (33)$$

Note that the optimal relaxation parameter  $\gamma_{\text{opt}}$  in realistic systems will be influenced by SNR and the receiver location. However, based on the analysis above, we can observe that

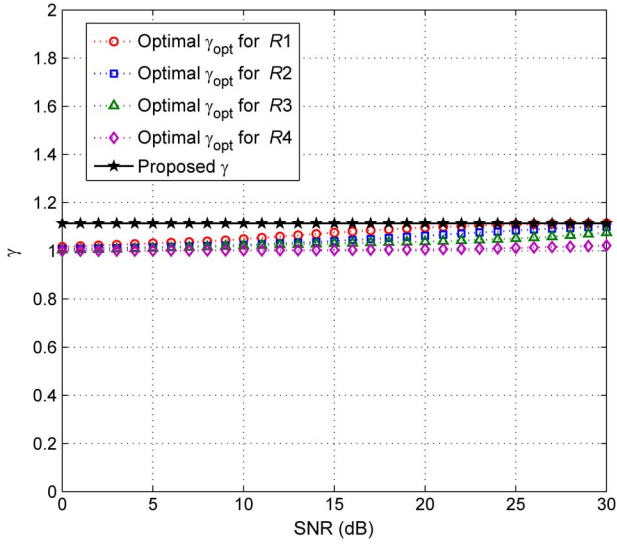


Fig. 4. Comparison between the proposed  $\gamma$  and the optimal  $\gamma_{\text{opt}}$  where  $N_t \times N_r = 16 \times 144$ , and the receiver is located at different places  $R_1$ ,  $R_2$ ,  $R_3$ , and  $R_4$  within the room.

such influence is negligible. To verify this conclusion, we locate the receiver at different places within the room as illustrated in Fig. 3, and Fig. 4 shows the comparison between the proposed  $\gamma$  (33) and the optimal  $\gamma_{\text{opt}}$  (28) when the receiver is located at  $R_1$ ,  $R_2$ ,  $R_3$ , and  $R_4$ , respectively. We can observe from Fig. 4 that the gap between  $\gamma_{\text{opt}}$  and  $\gamma$  is within 0.1 in the whole SNR range, and it becomes smaller with the increasing SNR. This indicates that the proposed  $\gamma$  (33), which is independent of SNR and the receiver location, is very close to  $\gamma_{\text{opt}}$ , especially when SNR is high. It's worth pointing out that the small difference between  $\gamma_{\text{opt}}$  and  $\gamma$  can only induce a little larger number of iterations for SOR-based algorithm to converge, which will be demonstrated by simulation results in Section IV. Therefore, the complexity will be only slightly increased, and the overall complexity is still much lower than Neumann-based algorithm and the classical MMSE algorithm as shown in the following Section III-D.

#### D. Computational Complexity Analysis

Since the computational complexity is dominated by multiplication and division operations, in this part, we evaluate the complexity in terms of required number of multiplications and divisions.

It can be found from (14) that the computational complexity of the  $i$ th iteration of SOR-based algorithm originates from solving the linear equation. Considering the definition of  $\mathbf{D}$  and  $\mathbf{L}$  in (10) and (11), the solution can be presented as

$$\begin{aligned} \hat{s}_m^{(i+1)} &= (1 - \gamma)\hat{s}_m^{(i)} \\ &+ \frac{\gamma}{w_{m,m}} \left( \hat{y}_m - \sum_{k < m} w_{m,k} \hat{s}_k^{(i+1)} - \sum_{k > m} w_{m,k} \hat{s}_k^{(i)} \right), \\ m, k &= 1, 2, \dots, N_t, \end{aligned} \quad (34)$$

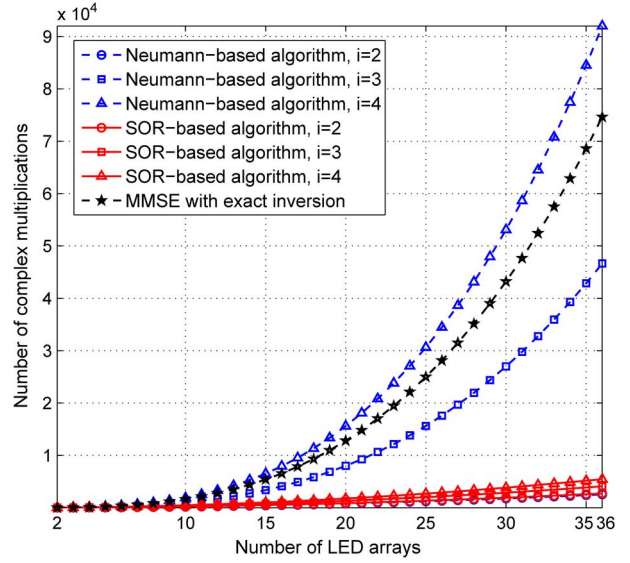


Fig. 5. Comparison of the computational complexity in terms of required number of multiplications.

where  $\hat{s}_m^{(i)}$ ,  $\hat{s}_m^{(i+1)}$ , and  $\hat{y}_m$  denote the  $m$ th element of  $\hat{\mathbf{s}}^{(i)}$ ,  $\hat{\mathbf{s}}^{(i+1)}$ , and  $\hat{\mathbf{y}}$  in (6), respectively, and  $w_{m,k}$  denotes the  $m$ th row and  $k$ th column entry of  $\mathbf{W}$ . The required number of multiplications to compute  $(1 - \gamma)\hat{s}_m^{(i)}$  and  $\frac{\gamma}{w_{m,m}}(\hat{y}_m - \sum_{k < m} w_{m,k} \hat{s}_k^{(i+1)} - \sum_{k > m} w_{m,k} \hat{s}_k^{(i)})$  is 1 and  $N_t + 1$ , respectively. Therefore, the computation of each element of  $\hat{\mathbf{s}}^{(i+1)}$  only requires  $N_t + 2$  times of multiplications. Since there are  $N_t$  elements in  $\hat{\mathbf{s}}^{(i+1)}$ , the overall required number of multiplications by the proposed SOR-based algorithm is  $i(N_t^2 + 2N_t)$ . In contrast, we can observe from (8) that Neumann-based algorithm has the overall complexity  $\mathcal{O}(N_t^2)$  when  $i = 2$  but  $\mathcal{O}((i - 2)N_t^3)$  when  $i \geq 3$  [15]. Besides, from (8) and (34), we can also observe that both SOR-based and Neumann-based algorithms are required to compute the diagonal matrix  $\mathbf{D}^{-1}$ . Thus, both algorithms involve  $N_t$  times of divisions, which is much lower than  $\mathcal{O}(N_t^2)$  required by MMSE algorithm with exact matrix inversion.

Fig. 5 compares the computational complexity in terms of required number of multiplications between the recently proposed Neumann-based algorithm [15] and our SOR-based algorithm, whereby the classical MMSE algorithm with exact matrix inversion is also included as a baseline for comparison. We can conclude from Fig. 5 that Neumann-based algorithm has lower complexity than MMSE algorithm when  $i \leq 3$ , especially when  $i = 2$  with the complexity  $\mathcal{O}(N_t^2)$ . However, when  $i \geq 4$ , its complexity is even higher than that of MMSE algorithm. To ensure the approximation performance, usually a large value of  $i$  is required (as will be verified later in Section IV). This means the overall complexity of Neumann-based algorithm is almost the same as that of MMSE algorithm, although it requires a much smaller number of divisions, which is preferred for hardware implementation. In contrast, we can observe that the proposed SOR-based algorithm requires the same number of divisions as that of Neumann-based algorithm, and its complexity is  $\mathcal{O}(N_t^2)$  for an arbitrary number of iter-

TABLE I  
PERCENTAGE OF COMPLEXITY COMPARED WITH MMSE ALGORITHM

|         | Neumann-based algorithm [15] | Proposed SOR-based algorithm |
|---------|------------------------------|------------------------------|
| $i = 2$ | 3.9 %                        | 4.3 %                        |
| $i = 3$ | 62.5 %                       | 6.4 %                        |
| $i = 4$ | 123 %                        | 8.5 %                        |
| $i = 5$ | 183 %                        | 10.6 %                       |

ations. Table I shows the percentage of complexity of SOR-based and Neumann-based algorithms compared with MMSE algorithm. We can observe that the proposed SOR-based algorithm can reduce the complexity by one order of magnitude since it can converge with a small number of iterations, as will be verified in Section IV. Moreover, as shown in Fig. 5 and Table I, larger dimension of MIMO systems will lead to a more significant reduction in complexity, which means that the proposed SOR-based algorithm with low complexity is quite suitable for indoor large-scale optical MIMO systems.

Additionally, we can observe from (34) that the computation of  $\hat{s}_m^{(i+1)}$  utilizes  $\hat{s}_k^{(i+1)}$  for  $k = 1, 2, \dots, m-1$  in the current  $(i+1)$ th iteration and  $\hat{s}_l^{(i)}$  for  $l = m, m+1, \dots, N_t$  in the previous  $i$ th iteration. Then, two other benefits can be expected. Firstly, after  $\hat{s}_m^{(i+1)}$  has been obtained, we can use it to overwrite  $\hat{s}_m^{(i)}$ , which is useless in the next computation of  $\hat{s}_{m+1}^{(i+1)}$ . Consequently, only one storage vector of size  $N_t \times 1$  is required; Secondly, the solution to (14) becomes closer to the final solution  $\hat{s}$  with an increasing  $i$ , so  $\hat{s}_m^{(i+1)}$  can exploit the elements of  $\hat{s}_k^{(i+1)}$  for  $k = 1, 2, \dots, m-1$  that have already been computed in the current  $(i+1)$ th iteration to produce more reliable result than Neumann-based algorithm [15], which only utilizes all the elements of  $\hat{s}^{(i)}$  in the previous  $i$ th iteration. Thus, the required number of iterations to achieve certain detection accuracy becomes smaller. Based on these two special advantages, the overall complexity of the proposed SOR-based algorithm can be reduced further.

#### IV. SIMULATION RESULTS

To evaluate the performance of the proposed SOR-based algorithm, we provide the BER simulation results compared with the recently proposed Neumann-based algorithm [15]. The BER performance of the classical MMSE algorithm with complicated but exact matrix inversion is also included as the benchmark for comparison. We consider the typical indoor large-scale optical MIMO with  $N_t \times N_r = 16 \times 144$ . For simplicity but without loss of generality, the modulation scheme of non-return to zero on-off keying (NRZ-OOK), which has been usually considered for wireless optical communications [3]–[5], is adopted. The channel model described in Section II is considered here, and the parameters used for simulation are summarized in Table II.

Fig. 6 shows the BER performance comparison between SOR-based algorithm with the optimal relaxation parameter  $\gamma_{\text{opt}}$  and the proposed relaxation parameter  $\gamma$  (33), where the receiver is located at  $R1$  as shown in Fig. 3, and  $i$  denotes the number of iterations. We can observe from Fig. 6 that

TABLE II  
PARAMETERS FOR INDOOR OPTICAL MIMO

| Parameter  | Value                      |
|--|----------------------------|
| Room size ( $L \times W \times H$ )                | 5m $\times$ 5m $\times$ 3m |
| Number of LED arrays                               | 4 $\times$ 4               |
| Number of LEDs per array                           | 30 $\times$ 30             |
| Distance between each array of LEDs                | 1m                         |
| Distance between LED in an array                   | 1cm                        |
| LED size   | 0.59cm $\times$ 0.59cm     |
| Light of LED                                       | white                      |
| Average transmitted power per LED                  | 10mW                       |
| Vertical distance from ceiling to imaging receiver | 2.15m                      |
| Number of photodetectors                           | 144                        |
| Image lens diameter                                | 0.44cm                     |
| Receiver FOV $\psi_c$ (semi-angle)                 | 63 degree                  |
| Refractive index of optical concentrator $n$       | 1.5                        |

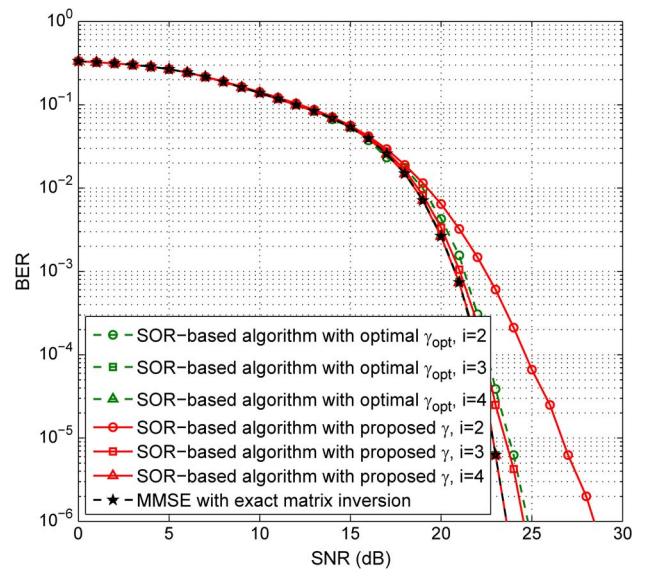


Fig. 6. BER performance of SOR-based algorithm with the optimal  $\gamma_{\text{opt}}$  and the proposed  $\gamma$ , where  $N_t \times N_r = 16 \times 144$  and the receiver is located at  $R1$ .

the optimal relaxation parameter  $\gamma_{\text{opt}}$  can guarantee a faster convergence rate than the proposed relaxation parameter  $\gamma$ . However, the difference of convergence rate is not obvious, since the proposed  $\gamma$  only induced one more iteration to converge, i.e.,  $i = 3$  for  $\gamma_{\text{opt}}$  and  $i = 4$  for  $\gamma$ . Therefore, when we use the proposed  $\gamma$  instead of  $\gamma_{\text{opt}}$  which varies with the receiver location and SNR, the complexity for signal detection will be only slightly increased, and the overall complexity is still much lower than Neumann-based algorithm and the classical MMSE algorithm as analyzed in Section III-D. This implies that we can still choose the proposed  $\gamma$ , which is simple and independent of the receiver location and SNR, to ensure the reliable performance in practice.

Fig. 7 shows the BER performance comparison between Neumann-based algorithm [15] and the proposed SOR-based algorithm in an  $N_t \times N_r = 16 \times 144$  large-scale optical MIMO system, where the receiver is located at  $R1$  and the proposed  $\gamma$  is used. It is clear that when the number of iterations is small (e.g.,  $i = 2$ ), Neumann-based algorithm cannot converge, leading to the obvious loss in the BER performance, while

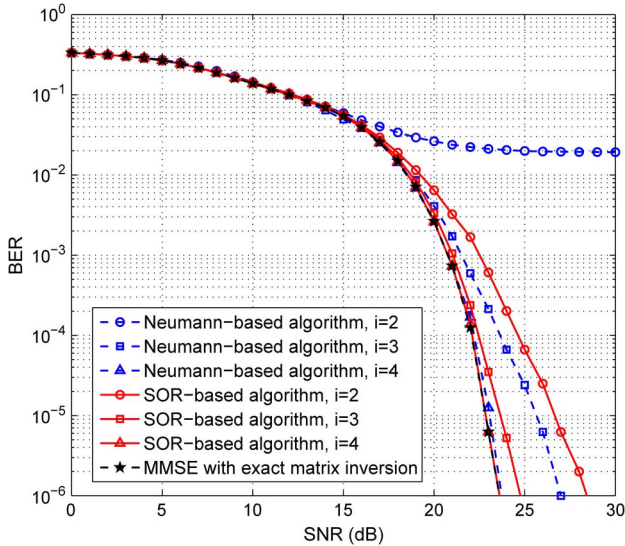


Fig. 7. BER performance comparison in an  $N_t \times N_r = 16 \times 144$  large-scale optical MIMO system, where the receiver is located at  $R1$  and the proposed  $\gamma$  is used.

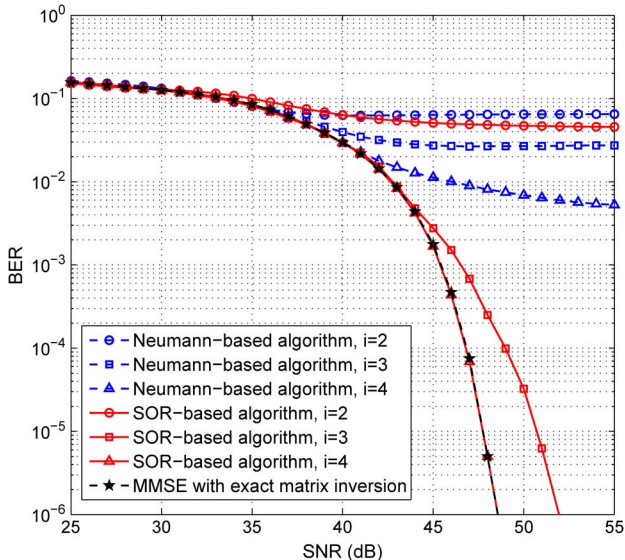


Fig. 8. BER performance comparison in an  $N_t \times N_r = 16 \times 144$  large-scale optical MIMO system, where the receiver is located at  $R3$  and the proposed  $\gamma$  is used.

SOR-based algorithm can achieve much better performance. As the number of iterations increases, the BER performance of both algorithms improves. However, when the same iteration number  $i$  is used, the proposed SOR-based algorithm outperforms Neumann-based algorithm. For example, when  $i = 3$ , the required SNR to achieve the BER of  $10^{-6}$  by SOR-based algorithm is 24.8 dB, while Neumann-based algorithm requires the SNR of 27 dB.

Fig. 8 shows the BER performance comparison in an  $N_t \times N_r = 16 \times 144$  large-scale optical MIMO system, where the receiver is located at  $R3$  as shown in Fig. 3 and the proposed  $\gamma$  is used. Comparing Figs. 7 and 8, we can observe that

when the receiver moves towards the room edges, all of the BER performance of MMSE, SOR-based and Neumann-based algorithms becomes worse. This is caused by the fact that when the receiver moves outwards, its distance and the angle of incidence to most LED arrays become large, leading to the reduced received signal power and the deteriorated BER performance. Meanwhile, the convergence rate of SOR-based algorithm is also slightly affected, since the optimal relaxation parameter will be a little different when the receiver location is changed as shown in Fig. 4. However, the proposed SOR-based algorithm can still converge with a small number of iterations even when the receiver is located at the room edges (i.e.,  $i = 4$  for both  $R1$  and  $R3$  to ensure the near-optimal performance), while Neumann-based algorithm can hardly converge when the receiver moves outwards. That indicates that the proposed SOR-based algorithm is more robust to the variation of receiver location.

Additionally, as it has been verified that MMSE algorithm can approach the performance of the optimal ML algorithm in large-scale MIMO systems [6], while the simulation results demonstrate that the proposed SOR-based algorithm can achieve the exact performance of MMSE algorithm with a small number of iterations, i.e.,  $i = 4$  in Figs. 7 and 8, we can infer that the proposed SOR-based algorithm can approach the same diversity order of the optimal ML algorithm as has been analyzed in [28].

## V. CONCLUSION

In this paper, we have proposed a low-complexity signal detection algorithm based on SOR method, which can achieve the near-optimal performance of the classical MMSE algorithm without complicated matrix inversion. We have analyzed the performance of SOR-based algorithm from three aspects. At first, we proved that SOR-based algorithm is convergent when the relaxation parameter  $\gamma$  satisfies  $0 < \gamma < 2$ . Then we proved that SOR-based algorithm with the optimal relaxation parameter can achieve a faster convergence rate than Neumann-based algorithm. At last, we proposed a simple quantified relaxation parameter independent of the receiver location and SNR to guarantee the performance of SOR-based algorithm in practice. It is shown that SOR-based algorithm can reduce the complexity from  $\mathcal{O}(N_t^3)$  to  $\mathcal{O}(N_t^2)$ . Simulation results demonstrate that the proposed SOR-based algorithm can achieve the exact performance of the classical MMSE algorithm with a small number of iterations, i.e.,  $i = 4$  for  $N_t \times N_r = 16 \times 144$  large-scale optical MIMO systems. Moreover, the idea of utilizing the SOR method to efficiently realize matrix inversion with low complexity can be extended to other signal processing problems involving matrix inversion, such as precoding in large-scale optical MIMO systems.

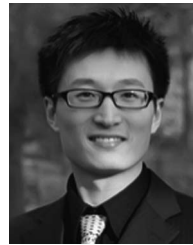
## REFERENCES

- [1] D. Kedar and S. Arnon, "Urban optical wireless communication networks: The main challenges and possible solutions," *IEEE Commun. Mag.*, vol. 42, no. 5, pp. S2–S7, May 2004.
- [2] A. H. Azhar, T. A. Tran, and D. O'Brien, "Demonstration of high-speed data transmission using MIMO-OFDM visible light communications," in *Proc. IEEE GLOBECOM*, Dec. 2010, pp. 1052–1056.

- [3] Z. Ghassemlooy, W. Popoola, and S. Rajbhandari, *Optical Wireless Communications: System and Channel Modelling With MATLAB*. Boca Raton, FL, USA: CRC Press, 2012.
- [4] L. Zeng *et al.*, "High data rate multiple input multiple output (MIMO) optical wireless communications using white LED lighting," *IEEE J. Sel. Areas Commun.*, vol. 27, no. 9, pp. 1654–1662, Sep. 2009.
- [5] T. Fath and H. Haas, "Performance comparison of MIMO techniques for optical wireless communications in indoor environments," *IEEE Trans. Commun.*, vol. 61, no. 2, pp. 733–742, Feb. 2013.
- [6] T. L. Marzetta, "Noncooperative cellular wireless with unlimited numbers of base station antennas," *IEEE Trans. Wireless Commun.*, vol. 9, no. 11, pp. 3590–3600, Nov. 2010.
- [7] H. Ngo, E. Larsson, and T. Marzetta, "Energy and spectral efficiency of very large multiuser MIMO systems," *IEEE Trans. Commun.*, vol. 61, no. 4, pp. 1436–1449, Apr. 2012.
- [8] D. Tsonev, S. Sinanovic, and H. Haas, "Practical MIMO capacity for indoor optical wireless communication with white LEDs," in *Proc. IEEE VTC Spring*, May 2013, pp. 1–5.
- [9] F. Rusek *et al.*, "Scaling up MIMO: Opportunities and challenges with very large arrays," *IEEE Signal Process. Mag.*, vol. 30, no. 1, pp. 40–60, Jan. 2013.
- [10] D. Gesbert, M. Shafi, D. Shiu, P. J. Smith, and A. Naguib, "From theory to practice: An overview of MIMO space-time coded wireless systems," *IEEE J. Sel. Areas Commun.*, vol. 21, no. 3, pp. 281–302, Mar. 2003.
- [11] B. Hassibi and H. Vikalo, "On the sphere-decoding algorithm I. Expected complexity," *IEEE Trans. Signal Process.*, vol. 53, no. 8, pp. 2806–2818, Aug. 2005.
- [12] L. G. Barbero and J. S. Thompson, "Fixing the complexity of the sphere decoder for MIMO detection," *IEEE Trans. Wireless Commun.*, vol. 7, no. 6, pp. 2131–2142, Jun. 2008.
- [13] N. Srinidhi, T. Datta, A. Chockalingam, and B. S. Rajan, "Layered tabu search algorithm for large-MIMO detection and a lower bound on ML performance," *IEEE Trans. Commun.*, vol. 59, no. 11, pp. 2955–2963, Nov. 2011.
- [14] T. Datta, N. Srinidhi, A. Chockalingam, and B. S. Rajan, "Random-restart reactive tabu search algorithm for detection in large-MIMO systems," *IEEE Commun. Lett.*, vol. 14, no. 12, pp. 1107–1109, Dec. 2010.
- [15] M. Wu *et al.*, "Large-scale MIMO detection for 3GPP LTE: Algorithms and FPGA implementations," *IEEE J. Sel. Topics Signal Process.*, vol. 8, no. 5, pp. 916–929, Oct. 2014.
- [16] A. Björck, *Numerical Methods for Least Squares Problems*. Philadelphia, PA, USA: SIAM, 1996.
- [17] J. M. Kahn *et al.*, "Imaging diversity receivers for high-speed infrared wireless communication," *IEEE Commun. Mag.*, vol. 36, no. 12, pp. 88–94, Dec. 1998.
- [18] T. Komine and M. Nakagawa, "Fundamental analysis for visible-light communication system using LED lights," *IEEE Trans. Consum. Electron.*, vol. 50, no. 1, pp. 100–107, Jan. 2004.
- [19] T. Q. Wang, Y. A. Sekercioglu, and J. Armstrong, "Analysis of an optical wireless receiver using a hemispherical lens with application in MIMO visible light communications," *J. Lightw. Technol.*, vol. 31, no. 11, pp. 1744–1754, Jun. 2013.
- [20] L. Dai, Z. Wang, and Z. Yang, "Spectrally efficient time-frequency training OFDM for mobile large-scale MIMO systems," *IEEE J. Sel. Areas Commun.*, vol. 31, no. 2, pp. 251–263, Feb. 2013.
- [21] F. Fernandes, A. E. Ashikhmin, and T. L. Marzetta, "Inter-cell interference in noncooperative TDD large scale antenna systems," *IEEE J. Sel. Areas Commun.*, vol. 31, no. 2, pp. 192–201, Feb. 2013.
- [22] I. B. Djordjevic, M. Arabaci, and L. L. Minkov, "Next generation FEC for high-capacity communication in optical transport networks," *J. Lightw. Technol.*, vol. 27, no. 16, pp. 3518–3530, Aug. 2009.
- [23] G. H. Golub and C. F. Van Loan, *Matrix Computations*. Baltimore, MD, USA: The Johns Hopkins Univ. Press, 2012.
- [24] J. Hoydis, S. T. Brink, and M. Debbah, "Massive MIMO in the UL/DL of cellular networks: How many antennas do we need?" *IEEE J. Sel. Areas Commun.*, vol. 31, no. 2, pp. 160–171, Feb. 2013.
- [25] R. Couillet *et al.*, *Random Matrix Methods for Wireless Communications*. Cambridge, MA, USA: Cambridge Univ. Press, 2011.
- [26] D. M. Young, *Iterative Solution of Large Linear Systems*. New York, NY, USA: Dover, 2013.
- [27] T. Chen, L. Liu, B. Tu, Z. Zheng, and W. Hu, "High-spatial-diversity imaging receiver using fisheye lens for indoor MIMO VLCs," *IEEE Photon. Technol. Lett.*, vol. 26, no. 22, pp. 2260–2263, Sep. 2014.
- [28] X. Jin and D. Cho, "Diversity analysis on transmit antenna selection for spatial multiplexing systems with ML detection," *IEEE Trans. Veh. Tech.*, vol. 62, no. 9, pp. 4653–4658, Nov. 2013.



**Xinyu Gao** (S'14) received the B.E. degree in communication engineering from Harbin Institute of Technology, Harbin, China, in 2014. He is currently working toward Ph.D. degree in electronic engineering with Tsinghua University, Beijing, China. His current research interests include physical-layer algorithms for massive MIMO systems, millimeter-wave communications, and optical wireless communications.



**Linglong Dai** (M'11–SM'14) received the B.S. degree from Zhejiang University, Hangzhou, China, in 2003; the M.S. degree (with the highest honors) from China Academy of Telecommunications Technology, Beijing, China, in 2006; and the Ph.D. degree (with the highest honors) from Tsinghua University, Beijing, in 2011. From 2011 to 2013, he was a Post-doctoral Fellow with the Department of Electronic Engineering, Tsinghua University. Since July 2013, he has been an Assistant Professor with the same department. His research interests are in wireless communications with the emphasis on OFDM, MIMO, synchronization, channel estimation, multiple-access techniques, and wireless positioning.



**Yuting Hu** (S'14) is currently working toward the B.S. degree in electronic engineering with the Department of Electronic Engineering, Tsinghua University, Beijing, China. Her current research interests include linear and nonlinear signal detection algorithms for massive MIMO systems and optical wireless communications. She was a recipient of the first-class scholarship of Tsinghua University in 2013 and the Science and Technology Innovation Award of Tsinghua University in 2014.



**Yu Zhang** (M'07–SM'12) received the B.E. and M.S. degrees in electronics engineering from Tsinghua University, Beijing, China, in 1999 and 2002, respectively, and the Ph.D. degree in electrical and computer engineering from Oregon State University, Corvallis, OR, USA, in 2006. In 2007, he was an Assistant Professor with the Research Institute of Information Technology, Tsinghua University, for eight months. He is currently an Associate Professor with the Department of Electronic Engineering, Tsinghua University. His current research interests include the performance analysis and detection schemes for MIMO-OFDM systems over doubly selective fading channels, transmitter and receiver diversity techniques, and channel estimation and equalization algorithm.



**Zhaocheng Wang** (SM'10) received the B.S., M.S., and Ph.D. degrees from Tsinghua University, Beijing, China, in 1991, 1993, and 1996, respectively. From 1996 to 1997, he was a Postdoctoral Fellow with Nanyang Technological University, Singapore. From 1997 to 1999, he was with Oki Techno Centre (Singapore) Pte Ltd. as a Research Engineer and then as a Senior Engineer. From 1999 to 2009, he was with SONY Deutschland GmbH as a Senior Engineer and then as a Principal Engineer. He is currently a Professor with the Department of Electronic Engineering, Tsinghua University. His research areas include wireless communications, digital broadcasting, and millimeter-wave communications. He is a Fellow of The Institution of Engineering and Technology. He has served as a Technical Program Committee Cochair/Member of many international conferences.